Hindawi Publishing Corporation
Shock and Vibration
Volume 2015, Article ID 423898, 14 pages
http://dx.doi.org/10.1155/2015/423898

Research Article

A PSO Driven Intelligent Model Updating and Parameter Identification Scheme for Cable-Damper System

Danhui Dan,[1] Yanyang Chen,[2] and Bin Xu[1]

[1]*Department of Bridge Engineering, Tongji University, Shanghai 200092, China*
[2]*Henan Provincial Communications Planning Survey & Design Institute Co., Ltd., Zhengzhou 450000, China*

Correspondence should be addressed to Danhui Dan; dandanhui@tongji.edu.cn

Received 15 February 2015; Revised 20 May 2015; Accepted 18 June 2015

Academic Editor: Miguel Neves

The precise measurement of the cable force is very important for monitoring and evaluating the operation status of cable structures such as cable-stayed bridges. The cable system should be installed with lateral dampers to reduce the vibration, which affects the precise measurement of the cable force and other cable parameters. This paper suggests a cable model updating calculation scheme driven by the particle swarm optimization (PSO) algorithm. By establishing a finite element model considering the static geometric nonlinearity and stress-stiffening effect firstly, an automatically finite element method model updating powered by PSO algorithm is proposed, with the aims to identify the cable force and relevant parameters of cable-damper system precisely. Both numerical case studies and full-scale cable tests indicated that, after two rounds of updating process, the algorithm can accurately identify the cable force, moment of inertia, and damping coefficient of the cable-damper system.

1. Introduction

The cable force is an important mechanics parameter of cable-stayed bridges and other cable structures. It is also an important reference for evaluating the operation status of this type of structure. Thus, the precise measurement of the cable force is an important part of structural health monitoring of cable structures. The cable force measurement method based on environmental vibration has become the most commonly used method by engineers because of its convenience, ease of use, and practicality. This method indirectly obtains the cable force by identifying frequencies from the vibration measurement data and establishing the relationship between the frequency and cable force [1, 2]. Under the condition of a taut string, this precise relationship can be transformed into an explicit formula of a taut string cable force. However, under normal circumstances where the bending stiffness of the cables, sag, and boundary conditions should be considered, errors would occur if this type of formula is employed to identify the cable force [3]. Thus, many researchers have been focusing on reducing these errors. These researches have two main approaches. One is to establish a more precise cable force-frequency expression. For example, Ni et al. established a frequency-cable force relationship that considers the sag and bending stiffness in 2002 [4]. Zui et al. [5] and Ren et al. [6] proposed a set of empirical formulas to identify the cable force based on the cable sag span ratio and grading of the bending stiffness in 1996. Ricciardi and Saitta established a dimensionless frequency equation by differentiating symmetric and asymmetric conditions in 2008 [7]. The authors of the present paper previously solved the zero root of this pair of equations by Newton's iteration method in 2014 to obtain the corrected cable force [8]. Another approach is to transform the calculation of the cable force into the identification of systems or to obtain the cable force by using an optimization method. Studies using this approach have been conducted by Geier et al. [9] and Kim and Park [10], Liwen et al. in 2012 [11], and Sun et al. in 2015 [12].

For long-span structures like cable-stayed bridges, the increased span makes cable dampers for vibration reduction an essential component of the cable-damper system. Because of the installation of external dampers, first-order derivative arguments of the cable lateral displacement appear in the vibration equation, and the single cable becomes a cable-damper system. This changes the dynamic characteristics of the structure and further affects the precision of the cable

force identification by the frequency formula method [13, 14]. Krenk [15] and Main and Jones [16, 17] have established sophisticated transcendental equations that describe the relationship between the cable modal frequency and cable parameters based on their research on the effect of dampers in a cable-damper system, but none of these equations can be used for solving the cable force because of the difficulty of solving for the numerical values.

Currently, there have been very few studies on how to identify the cable force and other cable parameters of the cable-damper system based on vibration measurement. The present paper presents a vibration measurement based cable force identification method suitable for cable-damper systems, which identify cable force and other parameters efficiently by cable finite element model updating approach driven by a novel stochastic search algorithm, namely, particle swarm optimization (PSO). The influences of the main parameters of the cable-damper system on the cable force error were examined through simulations, and reasonable guidelines for using this method were established.

2. Finite Element Model of Stay Cable Considering Stiffness, Sag, and Boundary Conditions

2.1. Finite Element Model of Stay Cable. It is difficult to establish a formula to solve for the cable force analytically when damper is added, especially when the bending stiffness, sag, and boundary conditions of the actual cables are all considered. Finite element methods are suitable for any complex cable structure and can provide accurate solutions with regard to the dynamic characteristics of relevant structures for cables.

For a cable-damper system where the above factors are considered, as shown in Figure 1, the finite element model requires the precise static equilibrium configuration of the cables to be determined first, which means that the sag effect must be considered. When the strain is small and the bending stiffness of cables is neglected, the precise expression of the cable equilibrium position is as follows:

$$y = \frac{H}{\rho g}\left[\cosh\left(\frac{\rho g l}{2H}\right) - \cosh\frac{\rho g}{H}\left(\frac{l}{2} - x\right)\right], \quad (1)$$

where H is the horizontal tension, ρ is the linear density, and l is the horizontal distance between the two anchoring ends of the cables. Depending on the cable length and boundary conditions, if the tangential angle is small along the cable length (i.e., $\theta \approx 0$), then

$$H\frac{d^2 y}{dx^2} = -\rho g\frac{ds}{dx} \approx -\rho g. \quad (2)$$

The shape of the cable's equilibrium position can be described by the following parabolic expression:

$$y = -\frac{\rho g}{2H}x(x - l). \quad (3)$$

In practical applications, the relative error of results obtained from these two curves is less than 1%, and the follow-up calculation can be conducted with quadratic parabolic functions.

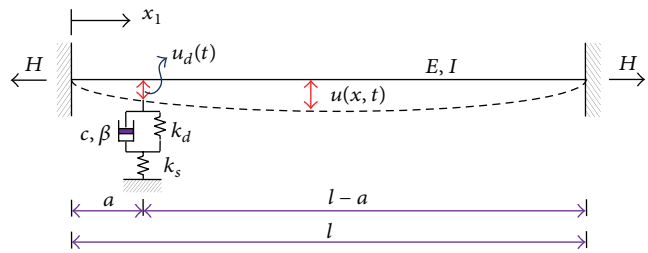

Figure 1: Cable-damper system considering various factors.

Based on the finite element method, the cable is divided into several sections according to the configuration after the cable's deformation, and the active position of the damper should be one of the dividing nodes. This makes each divided section into a simple cable segment and allows the cable-damper system to be divided into multiple elements. An elemental stiffness matrix is then established considering the geometric nonlinearity of the axial force and the effect of the bending moment. When the strain is small, the geometric stiffness matrix K_σ of the cable element can be determined by the elasticity theory:

$$K_\sigma = K_{\sigma,N_1} + K_{\sigma,N_2} + K_{\sigma,M_1} + K_{\sigma,M_2}, \quad (4)$$

where K_{σ,N_1} and K_{σ,N_2} are the axial force stiffness matrices and K_{σ,M_1} and K_{σ,M_2} are the bending moment stiffness matrices. Their expressions are given in Appendix. The element stiffness matrix of the cable element can be expressed by the following formula:

$$K = K_e + K_\sigma, \quad (5)$$

where K_e is the elasticity stiffness matrix, which is expressed in the appendix.

The damper element can be modeled with suitable components. K, M, and C are the global stiffness matrix, global mass matrix, and global damping matrix, respectively, for assembling the cable elements and applying the boundary conditions. Through eigenvalue analysis on this FEM model, the modal frequencies of the system can be calculated.

2.2. FEM Model Verification and FEM Model Updating Problem. To verify the model, a full-scale cable experiment was conducted in a cable factory. The cable frequency was obtained by spectrum analysis of the acceleration signals from the full-scale vibration experiment under environmental excitation. The rationality of the finite element model was preliminary and roughly verified through a comparison of the calculated and measured frequencies.

The parameters of the full-scale cable were as follows: a linear density of 96.85 kg/m, cable length of 95 m, initial cable force of 1460 kN, and cross-sectional area of 0.013 m^2. Both ends were anchored. Figure 2 shows a drawing of the layout for the experiment. During the experiment, four acceleration transducers were placed 2, 7, 12, and 17 m from the anchor

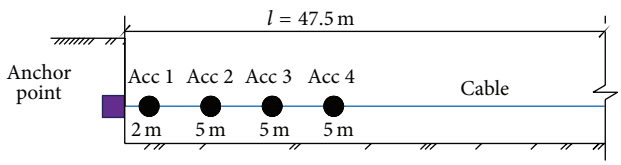

Figure 2: Layout of full-scale cable experiment.

end and given serial numbers of 1, 2, 3, and 4, respectively. No artificial excitation or external dampers were involved in the experiment, and only the vibration signal of the cable under the environmental excitation was measured. The duration of the experiment was set to 20 min, and the sampling frequency was 25.6 Hz.

Figure 3 shows the acceleration power spectral density obtained from spectrum analysis of the acceleration signal at points 3 and 4. Both the calculated and measured frequencies of the first and second modes of showed multiple relationships. The calculated and experimental fundamental frequencies were 0.8113 and 0.875 Hz, respectively, and the relative error was 7.28%. This indicates that this finite element model basically reflected the conditions of the full-scale cable, and the difference in the fundamental frequency was mainly due to the difference in the parameters of the cable calculation model and full-scale cable. That is the right difference for model updating to eliminate. Thus, precise simulation of the cable by the cable finite element model can be realized by updating the parameters of this model.

The measure of this difference can be described by the objective function f, which can be expressed as a function of the cable calculation model parameter $\mathbf{p}$ and full-scale cable parameter $\mathbf{p}^*$:

$$f = F_p(\mathbf{p}, \mathbf{p}^*) = \sqrt{\frac{1}{n-k+1}\sum_{i=k}^{n}\left(f_{i,\text{fem}} - f_{i,\text{test}}\right)^2}, \quad (6)$$

where $f_{i,\text{fem}}$ and $f_{i,\text{test}}$ represent the modal frequency obtained from the finite element analysis at the ith mode and the measured frequency for the corresponding mode. n is the total number of frequencies which can be detected. The mode order k in the calculation can be determined from the spectrum of the measured signal. Thus, the identification of the cable force and other parameters can be transformed into a form of classic model updating problem or math optimization problem:

$$\mathbf{p}^{\text{opt}} = \arg\min_{\mathbf{p}\to\mathbf{p}^*}\left(F_p(\mathbf{p}, \mathbf{p}^*)\right). \quad (7)$$

The optimal solution of the above optimization problem can be solved under the constraint condition:

$$\mathbf{p}^L \le \mathbf{p} \le \mathbf{p}^U \quad (8)$$

in its feasible region, where $\mathbf{p}^L$ and $\mathbf{p}^U$ are the lower and upper bounds of the feasible region of the cable parameter. The element corresponding to the cable force in the vector of optimal solution $\mathbf{p}^{\text{opt}}$ is the identified result for the cable force.

2.3. Sensitivity Analysis of Cable Parameters. The parameters of the cable-damper system to be updated include the cable force, bending stiffness, extension stiffness, cable length (i.e., distance between the coordinates of the upper and lower anchor points), linear density of the cable, boundary conditions, and size of the lateral damper. Some of these parameters are known and do not need to be updated, some are still unknown and need to be updated, and some are unknown but do not need to be updated. The preliminary difficulty lies in selection of the reasonable updating variables when pursuing a successful model updating effect. The good selection of the parameters to be updated leads to both the efficiency and the reasonability of the model updating. The parameters of the cable-damper system to be updated can be selected by sensitivity analysis of the cable parameters.

A sensitivity analysis was performed on the cable parameters based on the above updating objective functions. The difference sensitivity vector $\mathbf{s}$ of the objective function for cable parameters can be defined as

$$\mathbf{s} = \frac{\Delta F_p(\mathbf{p}, \mathbf{p}^*)}{\Delta \mathbf{p}}. \quad (9)$$

For convenience, the sensitivity analysis in the above formula can be substituted for by the dimensionless relative sensitivity of the cable modal frequency to the system parameters $S_{i,j}$, which can be defined as the ratio between the relative error of the structure modal frequency caused by a change in the structure parameters and the relative variation in the structure parameters:

$$S_{i,j} = \frac{\left(f_i(p_j + \Delta p_j) - f_i(p_j)\right)/f_i(p_j)}{\Delta p_j / p_j}, \quad (10)$$

where $f_i(p_j)$ is the modal frequency of the ith mode when the structure parameter is p_j and Δp_j is the variation in the jth parameter.

Parameters such as the cable length, elastic modulus, linear density, and sectional area of the cable and the installation location of the damper were found to be easily determined from the material, geometric, and physical parameters of the cable-damper system. It was very difficult to precisely measure the cross-sectional moment of inertia of the cable, and the actual damping coefficient of the damper is affected by its installation quality. Thus, the parameters of the cable-damper system to be updated are cable force, cross-sectional moment of inertia, and damping coefficient.

The finite element model of the cable presented in Figure 2 was established, and the sensitivity of the first 10 modes of modal frequencies to the system parameters for the cable-damper system was analyzed. These parameters include the cable length, cable force, elastic modulus, linear density, damping coefficient, and cross-sectional moment of inertia of the cable. Figure 4 shows the sensitivity analysis results for the cable force, damping coefficient, cross-sectional moment of inertia, and elastic modulus. Table 1 presents the maximum sensitivity values of various mode frequencies.

The results in Figure 4 and Table 1 show that the modal frequency was highly sensitive to the cable length, cable

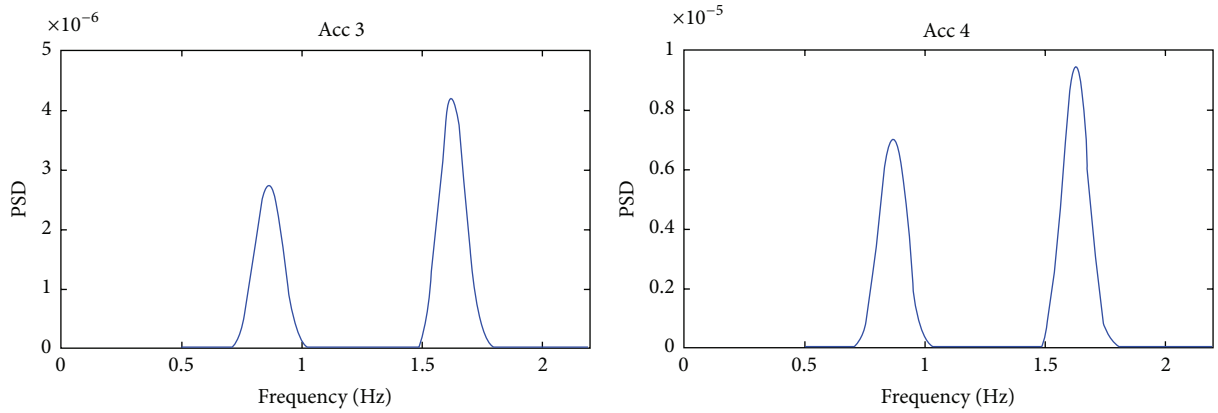

(a) (b)

Figure 3: Acceleration of power spectral densities of points 3 and 4 in full-scale cable experiment.

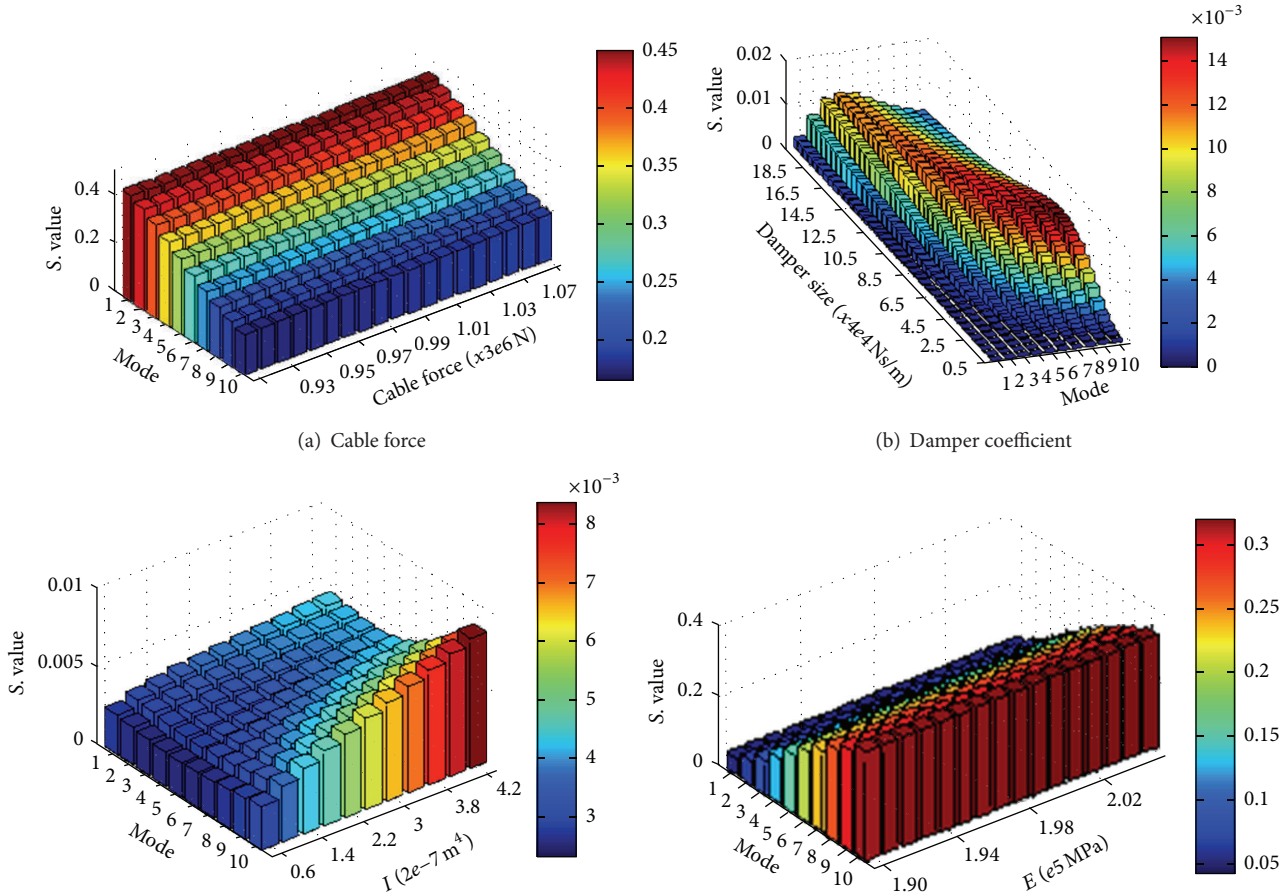

(a) Cable force

(b) Damper coefficient

(c) Moment of inertia

(d) Elastic modulus

Figure 4: Sensitivity of first 10 modes of modal frequencies of cable to cable parameters.

Table 1: Results of sensitivity analysis.

Parameter	Cable force (H)	Moment of inertia (I)	Cable length (L)	Elastic modulus (E)	Linear density (ρ)	Damping coefficient (c)
Max. sensitivity	0.4	0.004	−0.8	0.36	−0.5	0.001–0.01

force, and elastic modulus and was relatively low sensitive to the moment of inertia and damping coefficient of the cable. However, because cable length and elastic modulus are known physical quantities with low discreteness, they are not regarded as updating variables. As shown in Figures 4(c) and 4(d), although sensitivity to the moment of inertia is low, the product of the moment of inertia and the elastic modulus (i.e., sensitive to the bending stiffness) are very sensitive and significant to be chosen as an updating parameter. With comprehensive analysis, the cable force, cross-sectional moment of inertia, and damping coefficient of the damper were selected as the updating variables for the model updating of the cable-damper system.

3. PSO-Based Cable FEM Model Updating

3.1. Basic PSO Algorithm. The basic concept for a particle swarm comes from the migration and bunching of birds looking for food. A global random searching algorithm based on group intelligence was proposed that imitates and simulates these behaviors [18]. Kennedy and Eberhart proposed a simulation model of birds feeding based on the biologist Frank Heppner's model of birds. Their model allows the particle swarm to obtain the position of present step in the solution space at any time during their flying and the swarm to approach the target through information exchanges among individuals until the entire swarm reaches the destination. Thus, the optimal result of the swarm is obtained [19]. Since the original PSO algorithm is present, researchers continually introduced many new and more sophisticated PSO variants with an attempt to improve optimization performance. There are certain trends in that research; one is to make a hybrid optimization method using PSO combined with other optimizers [20]. Another research trend is to try to alleviate premature convergence, for example, by reversing or perturbing the movement of the PSO particles [21]; another approach to deal with premature convergence is the use of multiple swarms [22]. Finally, there are developments in adapting the behavioural parameters of PSO during optimization [23].

PSO needs few or no assumptions about the problem being optimized and can search very large spaces of candidate solutions. More specifically, PSO does not use the gradient of the problem being optimized, which means PSO does not require that the optimization problem be differentiable as is required by classic optimization methods such as gradient descent and quasi-Newton methods. PSO can therefore be used on complicated optimization problems that cannot be expressed explicitly and multiobjective problems.

The optimization problems have the objective function defined as (6) which requires an eigenvalue analysis done with a finite element model. The expression of gradient of (6) can in general be obtained numerically but usually it requires programming a subroutine to do it. In this particular case of a cable it is specially complicated due to the involved matrices of (4). The PSO algorithm is an easy-to-use approach and can be used to solve FEM model updating problems as present in this paper.

A basic frame of PSO algorithm can be described as follows.

In a n dimensional space, the particle swarm is assumed to be made of s particles, and every particle is flying at a certain speed. $X_i = (x_{i1}, x_{i2}, \ldots, x_{in})$ is assumed to be the current location of the particle i. $V_i = (v_{i1}, v_{i2}, \ldots, v_{in})$ is the current speed of the particle i. $P_i = (p_{i1}, p_{i2}, \ldots, p_{in})$ is the best location that the particle i has ever been at and is also the location with the best adaptive value that the particle i has ever been at. It is called the best individual location. (Unlike above, i represents the serial number of the particles. This definition continues to be applied below.)

$f(x)$ is assumed to be the optimized objective function, and common optimization matters can be transformed into the minimization of $f(x)$. Then, the best current location of the particle i is determined by the following method:

$$P_i(t+1) = \begin{cases} P_i(t), & \text{as } f(x_i(t+1)) \geq f(P_i(t)) \\ X_i(t+1), & \text{as } f(x_i(t+1)) < f(P_i(t)). \end{cases} \tag{11}$$

For particle swarms, $P_g(t)$ represents the best location that all particles have ever been, and it is called the best global location if marked with "g." This is determined as follows:

$$P_g(t) = \underset{P_i(t), i=1,\ldots,s}{\arg\min} \left(f(P_i(t))\right). \tag{12}$$

The evolution equation of the basic particle swarm algorithm can be described as

$$\begin{aligned} V_{ij}(t+1) &= V_{ij}(t) + c_1 r_{1j}(t)\left(p_{ij}(t) - x_{ij}(t)\right) \\ &\quad + c_2 r_{2j}(t)\left(p_{gj}(t) - x_{ij}(t)\right), \\ x_{ij}(t+1) &= x_{ij}(t) + V_{ij}(t+1). \end{aligned} \tag{13}$$

In the formula, j represents the dimension of the particle, $j = 0, 1, \ldots, i$ represents the serial number of the particles, t represents the evolution algebra, $r_{1j}(t)$ and $r_{2j}(t)$ are two mutually independent random functions, and c_1 and c_2 represent the acceleration constants. These constants are usually in the range of $[0, 2]$, and the above two independent random functions $r_{1j}(t)$ and $r_{2j}(t)$ are in the range of $[0, 1]$.

According to formula (13), the speed evolution of particles consists of three parts: the original speed term $V_{ij}(t)$, the correction term to consider the effect of the best location of the particle on the current location $c_1 r_{1j}(t)(p_{ij}(t) - x_{ij}(t))$ (i.e., individual cognition), and the correction considering the effect of the best location of the particle swarm on the current location $c_2 r_{2j}(t)(p_{gj}(t) - x_{ij}(t))$ (i.e., social cognition). The evolution of speed is determined by all three parts.

In the primary stage, after the swarm size s is set, the initial swarm location and initial speed can be obtained in the searching spaces $[-x_{\max}, x_{\max}]$ and $[-V_{\max}, V_{\max}]$ following a certain pattern (e.g., obeying the uniform distribution). Usually, $V_{\max} = \alpha x_{\max}$ and $0.1 \leq \alpha \leq 1.0$. If the value of the optimal solution can be predicted, this discrete value can

be selected as the seed of the particle swarm to form a swarm location that is near to or even includes the optimal solution. This would save the searching time of the calculation and allow the algorithm to quickly obtain the optimal solution [18].

3.2. Improved on PSO Algorithms. The particle swarm algorithm has few requirements for objective functions. It is easy to operate, and its optimization ability is high under certain circumstances. Thus, it has shown great potential as a random searching optimization algorithm. Particles in PSO gather towards the best locations of themselves and the neighborhood or swarm and form the rapid convergent of the particle swarm. Thus, they easily cause local extrema, premature convergence, or stabilization [19, 23]. The PSO performance naturally also depends on the algorithm parameters [24, 25]. Various improvement measures have been taken to overcome the above flaws, including partial escape techniques, neighborhood topology, parameter optimization selection, and mixed strategies.

As the focus here is on applied research, the performance of various measures or a comparison of the selected methods is outside the scope of this paper. However, some improvements were made to the existing PSO algorithm based on the optimization of specific multidimensional spaces to avoid local extrema, premature convergence, and so forth during the optimization of high-dimensional spaces. Different status update strategies can be used for the global optimal particles and other particles obtained after each flying step. As shown in Figure 5, the status of common particles is updated with formula (14). For current global optimal particles, the speed and direction at the next step are predicted with formula (15) based on the records of the neighboring two-step global optimal locations to realize a self-adapting partial searching ability:

$$P_g(t+1) = \frac{E_{\text{tol}} - f\left(P_g(t)\right)}{k_g(t)} + P_g(t). \tag{14}$$

In the formula, E_{tol} is the minimum tolerance value of the objective function and $k_g(t)$ is the estimated slope of the current global optimal performance curve, which can be expressed as follows:

$$k_g(t) = \frac{f\left(P_g(t)\right) - f\left(P_g(t-1)\right)}{P_g(t) - P_g(t-1)}. \tag{15}$$

The second improvement measure is to increase the escape speed of common particles when they are partially premature to improve the global searching ability.

3.3. Flowchart of Cable FEM Model Updating Driven by PSO. The minimum optimization as determined by the model updating objective function can be solved by many algorithms including genetic algorithms, simulated annealing, and PSO. Thus, the mechanical and physical parameters of the cable can be obtained. In this research, the optimal solution of the objective function was conducted by PSO algorithm. The flowchart of the model updating is shown in Figure 6.

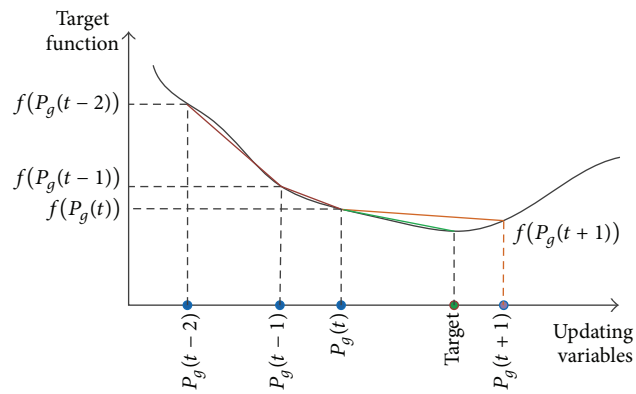

Figure 5: Adaptive state updating of global optimal particle.

4. Numerical Study

Three cable parameterization finite element models with dampers were established based on cable numbers B01, B11, and B17 of the Shanghai Yangtze River Bridge, and the model updating of the cable-damper system was studied with the proposed method to identify the cable force and other parameters. During the modeling, the damper was installed on the in plane, and the cable force was assumed to not change either before or after the installation of the damper. Because the anchoring end of the cable was stuck during the second phase of construction, a simulation with a rigid connection for the cable boundary condition was selected. Table 2 lists the basic parameters of the cables.

4.1. Accuracy of Algorithm. Based on the above research conclusions, the cable force, moment of inertia, and damping coefficient of the damper were selected as the updating variables. The finite element parameterization models were evaluated with the basic parameters given in Table 2 in a modal analysis, and the modal frequencies of the first five modes obtained were used as the measured modal parameters. A deviation was given to the three above parameters to be updated, and the finite element parameterization model was evaluated again. The calculated modal frequencies were obtained by modal analysis and substituted into formula (6) to obtain the value of the optimization objective function. Then, the automatic updating was performed by using PSO. Table 3 gives the operating parameters of the PSO updating algorithm.

The PSO algorithm needs to select a group of initial values for the updating variables. In this study, the initial values of cable forces were selected as the value calculated by frequency formula of taut string. The initial value of the cross-sectional moment of inertia was calculated from the circular section equivalent to the naked cable diameter. The initial value of the damping coefficient of damper was selected according to the nominal value of dampers. After several cycle iterations, the proposed PSO algorithm obtained satisfying optimization results for the cable force and damping coefficient but poor results for the cross-sectional moment of inertia. Figure 7

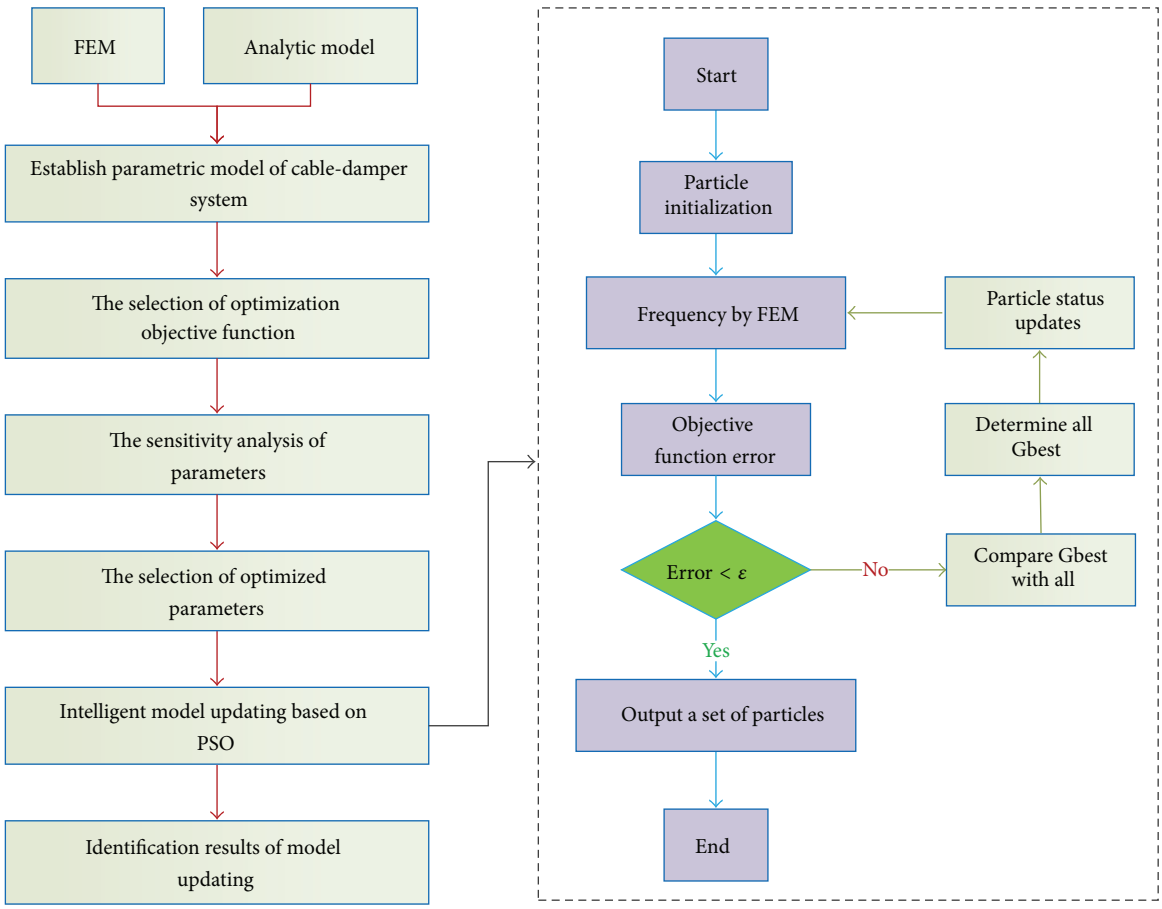

Figure 6: Flowchart of cable FEM model updating driven by PSO method.

Table 2: Simulation parameters for cables.

Cable SN	Cable length (m)	Sectional area (m^2)	Cross-sectional moment of inertia (m^4)	Linear density ($kg\,m^{-1}$)	Cable Force (kN)	Cable angle (°)	Damping coefficient ($N\,s\,m^{-1}$)	Height m
B01	100.0	$5.81e-3$	$3.9496e-7$	48.1	$3e3$	70.0	$4.0e4$	2.0
B11	300.0	$1.2970e-2$	$1.9436e-6$	106.4	$5.46e3$	28.0	$5.0e4$	6.0
B17	150.0	$1.0197e-2$	$1.2776e-6$	84.1	$4.5e3$	30.0	$5.0e4$	4.0

Table 3: Parameters of correction algorithm.

Name of algorithm	Iterative step	Number of swarms	Acceleration constant	Inertia weight	Number of dimensions
Improved PSO algorithms	100	60.0	3.0	$0.9 \rightarrow 0.4$	3

shows the evolutionary process of the objective function with the iterations. The updating results are given in Tables 4–6.

Figure 7 shows that the simulated cable B01 converged at the 45th steps of the iteration. The convergence speeds of cables B11 and B17 are similar to that of cable B01. The model updating results of the three simulated cables (see Tables 4–6) indicated that the cable force and damping coefficient of the numerical simulated cable showed a high identification precision. The identification precision of the cable force was within 0.5%, and the error of the identified damping coefficient was less than 2% compared with the actual value. The precision of cable moment of inertia was very low with a maximum error of nearly 60%.

To overcome this flaw, the identified cable force and damping coefficient were used as known values and act as an input of these three cable finite element models, together with other known parameters of cable-damper system. The moment of inertia was used as the only updating variable

Table 4: Model updating results for simulated cable B01.

Cable 1	Cable force (kN)	Cross-sectional moment of inertia (m^4)	Damping coefficient ($N\,s\,m^{-1}$)
Correction result	2993.143	$5.4e-7$	$4.0789e4$
Full-scale cable parameter	$3.0e3$	$3.9496e-7$	$4.0e4$
Relative error	−0.23%	36.72%	1.97%

Table 5: Model updating results for simulated cable B11.

Cable 2	Cable force (kN)	Cross-sectional moment of inertia (m^4)	Damping coefficient ($N\,s\,m^{-1}$)
Correction result	5476.563	$8.4e-7$	$4.94226e4$
Full-scale cable parameter	$5.46e3$	$1.9436e-6$	$5.0e4$
Relative error	0.3%	−56.78%	1.15%

Table 6: Model updating results for simulated cable B17.

Cable 3	Cable force (kN)	Cross-sectional moment of inertia (m^4)	Damping coefficient ($N\,s\,m^{-1}$)
Correction result	4489.550	$1.8e-6$	$5.0353e5$
Full-scale cable parameter	$4.5e3$	$1.2776e-6$	$5.0e5$
Relative error	−0.23%	40.89%	0.71%

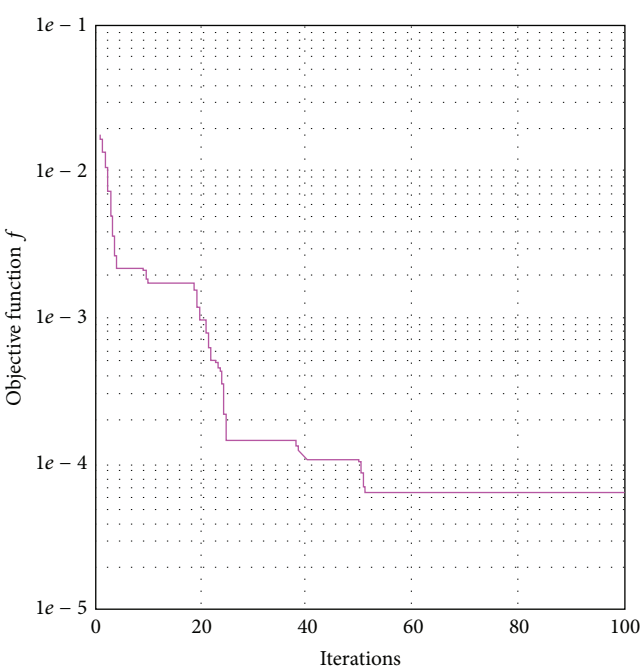

Figure 7: Iteration history of model updating objective function (cable B01).

to conduct a second round updating process. This time the proposed algorithm quickly met the conditions of convergence and obtained satisfying results. The relative error of the moment of inertia was reduced to less than 5%, as given in Table 7. This indicates that the moment of inertia of the cable can be predicted grossly with a general scope in first round updating and then be identified precisely through a second round updating process.

Table 7: Second updating result for moment of inertia (m^4).

Cable number	Cable 1	Cable 2	Cable 3
First correction result	$5.4e-7$	$8.4e-7$	$1.8e-6$
Second correction result	$4.0724e-7$	$1.9098e-6$	$1.2896e-6$
Parameter of finite element model	$3.9496e-7$	$1.9436e-6$	$1.2776e-6$
First relevant error	36.72%	−56.78%	40.89%
Second relevant error	3.11%	−1.74%	0.94%

4.2. Stability of Algorithms. Because the PSO algorithm is a kind of random searching algorithm, the results of a single updating process would also be random. Thus, in order to test the statistical stability of the proposed PSO algorithm, several repeated updating processes were conducted on the above cable B01 using identical configuration parameters to test the convergence rate of the proposed algorithm, the convergence objective function, and the quality of the convergence results. The same algorithm parameters in Table 3 are used. It can be seen from Figure 7 that the identified values of cable force and damping coefficient are fairly good when a target function reaches a value of 10^{-4}. However, to order to investigate the stability of the algorithm, we still set the maximum epoch of each updating round to 3000 steps and set the iteration termination condition to 10^{-5}. Fifty rounds of independent updating processes were conducted under this iteration termination condition. Figure 8 shows the descending process of the objective function during these 50 rounds of model

Table 8: Identification results.

Identification parameter	First cable force (kN)	First damping coefficient (N s m^{-1})	First cross-sectional moment of inertia (m^4)	Second correctional moment of inertia (m^4)
Correctional result	1.3927e3	2.7988e5	2.102e − 6	4.9159e − 6
Parameter of full-scale cable	1.4499e3	2.737e5	6.6783e − 6	6.6783e − 6
Relative error	−3.95%	2.26%	−68.52%	−26.39%

updating. All 50 rounds of the iteration process reached the value of 10^{-4} within 2000 steps, which means that the algorithm is stable within 2000 steps, and fairly good global optimal values can be obtained.

Figure 8 also indicates that the objective function in the final terminated iteration may not reach the global optimal value if the termination iteration step is set to be small number and the error of the updating parameter is relatively high. Thus, the results of the above multiple rounds of updating should be further investigated to discover the relationship between the objective function and the relative error of the updating variable at the relative small number; here, this number is set to 300. The relative error of the updating variable was defined as the ratio between the difference and the actual value.

Figure 9 shows the relationship curve between the relative errors of the objective function and the correction variables of the cable force, moment of inertia, and damping coefficient of the damper at the 300th iteration step. A good linear relationship can be found between the objective function value f and the relative errors of the optimization variables H, I, and c. Their respective regression relationships are given as follows:

$$\begin{aligned} e_H &= 14.3147 \times f - 0.00045213 \\ e_I &= 28.6342 \times f - 0.00099901 \\ e_c &= 14.7189 \times f - 0.00045679. \end{aligned} \tag{16}$$

Thus, the above formula can be substituted with the objective function value when a certain round of iteration is ended to estimate the error range of the updating variable.

5. Application to Real Cable-Damper System

5.1. Introduction of Real Cable Test. In order to verify the parameter identification of the model updating method for a real cable-damper system, a dynamic experiment was carried out on full-scale cables in same cable factory as mentioned before. In the experiment, the cable was stretched across the geosyncline horizontally with the two cable ends anchored. Displacement meters were installed at $L/2$ and $L/4$ of the cable as well as at the damper's position. Accelerometers were set up at $L/4$ and $3L/8$ of the cable. Figure 10 shows the layout of the experiment site and photos of the experiment. The parameters of the full-scale cable were as follows: a length of 95 m, a linear density of 60.19 kg/m, a diameter of 125 mm, and an elasticity modulus of 2.0×10^{11} Pa. The damper's position was 2.2 m from the left anchor point.

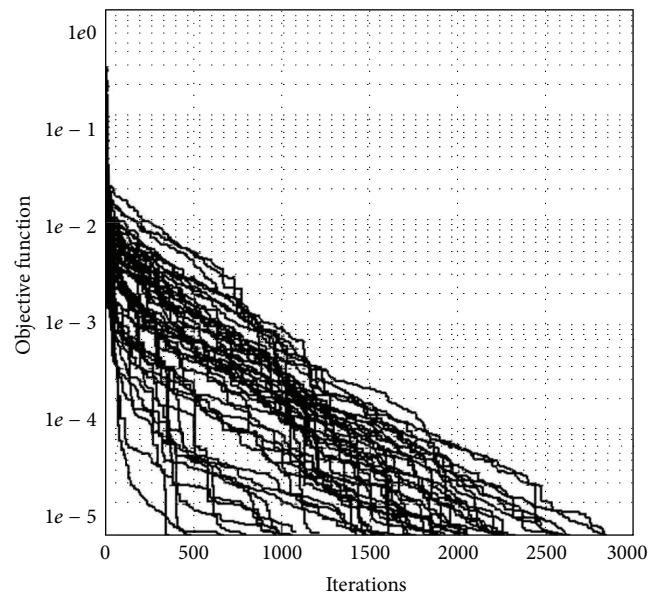

Figure 8: Multiple rounds of repeated tests of objective function.

5.2. The Results of Model Updating. The free decay oscillation test was conducted and recorded. The sampling frequency was 25.6 Hz, and each sampling time lasted 300 s. Figure 11 shows the acceleration record and its corresponding PSD of the cable-damper system. The frequencies of the first four modes were 0.8879, 1.676, 2.526, and 3.376 Hz.

The frequencies of the first four modes were regarded as the updating objective functions, and the PSO algorithm was adopted for the model updating. Table 8 provides the updating results.

The cable force of the cable-damper system identified after the first turn updating is 1.3927×10^6 N, which was less than the actual tensile force with an error of 3.95%. The damping coefficient was 2.7988×10^5 N s m^{-1} after the first turn updating and identification error is 2.26%. Both of these two parameters showed good precision. But the error on moment of inertia after the first turn updating is quite large. Therefore, the identified cable force and damper were plugged into the finite element model as known values, and the moment of inertia was updated again as the unknown updating variable. This time, the error was smaller but was still at a value of 26.39%. This is because the full-scale cable's moment of inertia was estimated under the assumption that the cable's section was made of homogeneous steel. However, the actual cable was formed from tied cable strands, and its actual moment of inertia was far smaller than that indicated

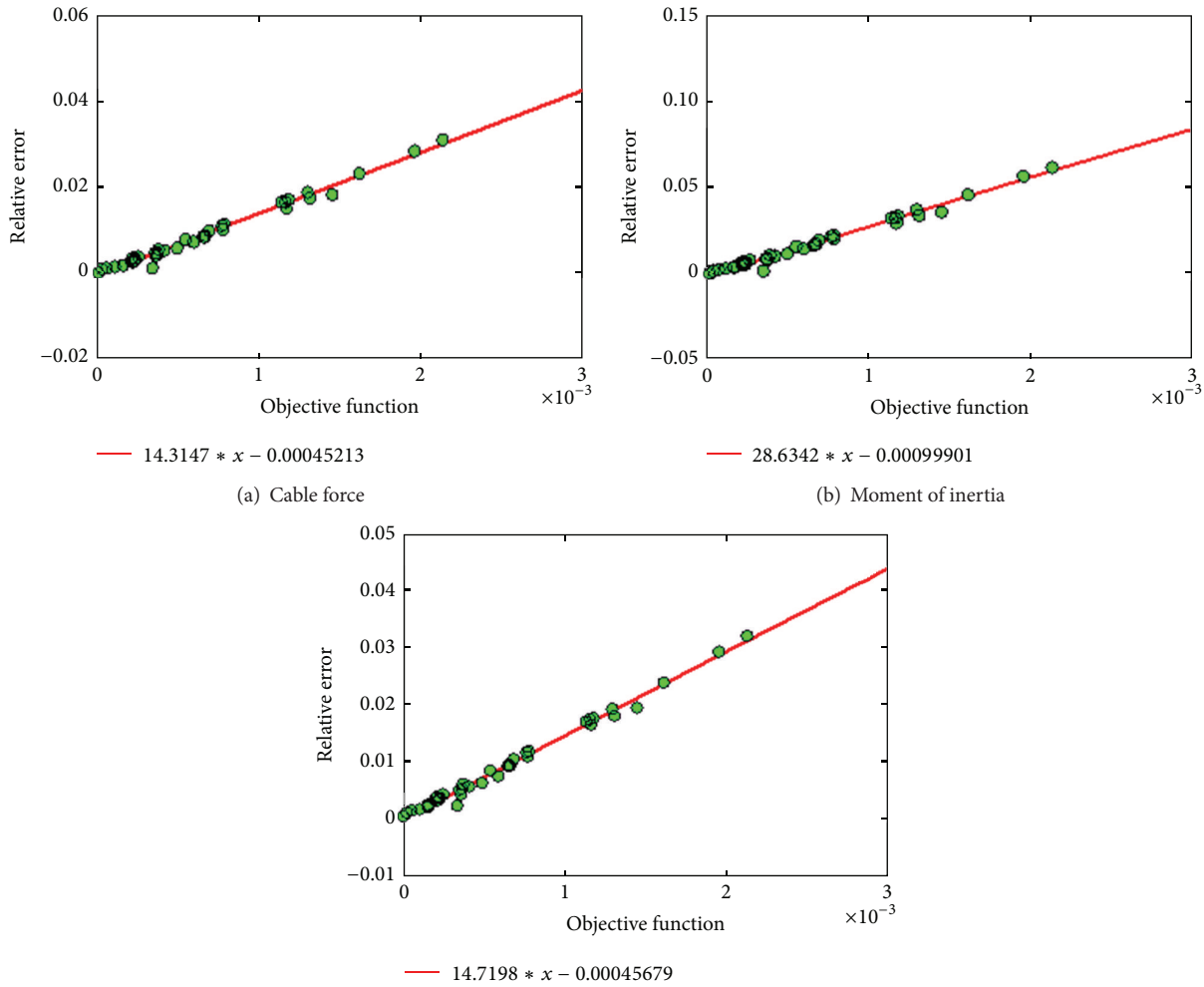

(a) Cable force

(b) Moment of inertia

(c) Damping coefficient

Figure 9: Relationship curves between relative errors of objective function and correction variables.

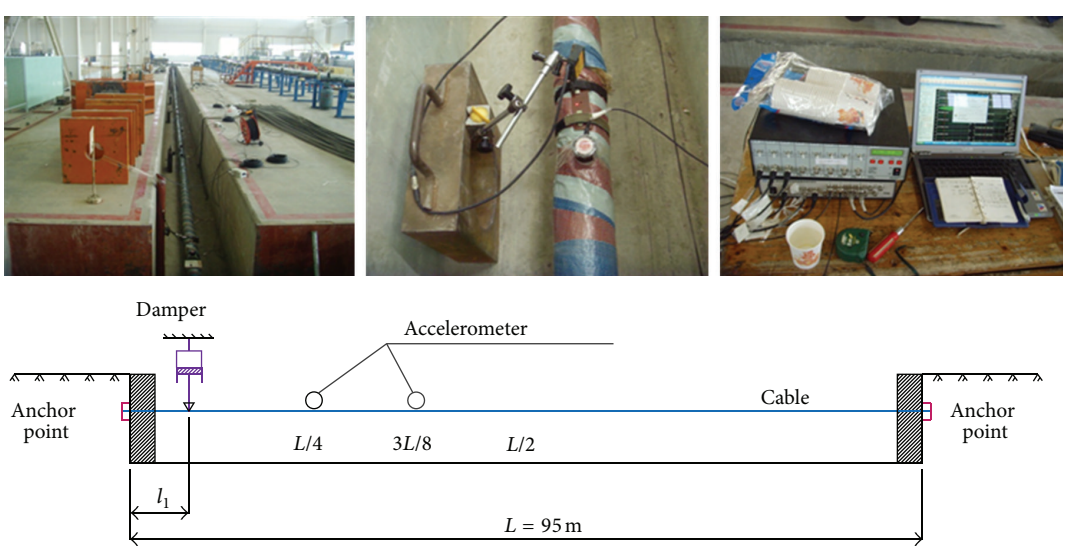

Figure 10: Real cable-damper system test in factory.

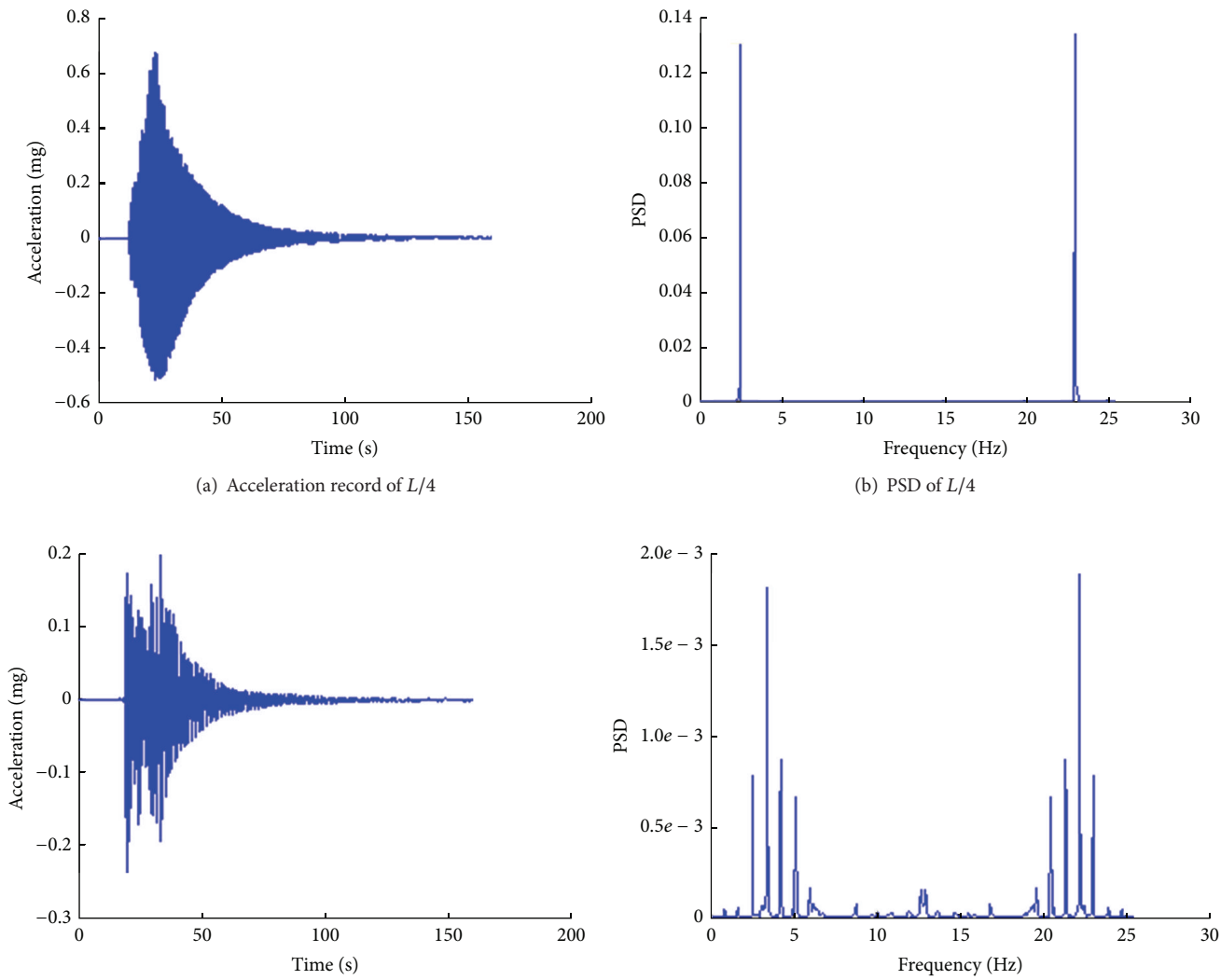

(a) Acceleration record of $L/4$

(b) PSD of $L/4$

(c) Acceleration record of $3/8L$

(d) PSD of $3/8L$

Figure 11: Acceleration record and PSD of full-scale cable experiment.

in the figure. Thus, it is believed that the identified moment of inertia is closer to the actual one of the cable than the value gotten in first turn updating process.

6. Conclusion

The precise measurement of the cable force is essential to understanding a bridge's internal forces. When an external damper is installed on a cable, the existing vibration method employed to identify the cable force and other parameters is quite imprecise. Particularly when some cable parameters are unknown, large identification errors for the cable force will be induced. The proposed model updating method for a cable-damper system driven by PSO algorithm can perform this optimization process and identify the basic mechanical parameters of the cable-damper system automatically and intelligently.

During the model updating, sensitivity analysis should be applied to select suitable updating variables; these include the cable force, damping coefficient, and moment of inertia. The numerical simulated case on cable model updating proves that PSO can be used to identify the cable force and damping coefficient of cable-damper system precisely. Precise identifications may also be obtained for the cable's moment of inertia after a second round of updating. The full-scale cable experiment revealed that the suggested identification scheme for cable parameters provides reliable and precise identification results. It can be concluded that proposed method is precise and reliable overall and thus can be regarded as a good identification scheme.

Appendix

The contributions to the stiffness matrix K in (5) can bewritten as in the following, which can be found in some

of FEM textbook which present the formulation for the geometric nonlinearity, like, for example, [26]

$$K_e = \begin{bmatrix} \frac{EA}{L} & 0 & 0 & -\frac{EA}{L} & 0 & 0 \\ 0 & \frac{12EI}{L^3} & \frac{6EI}{L^2} & 0 & -\frac{12EI}{L^3} & \frac{6EI}{L^2} \\ 0 & \frac{6EI}{L^2} & \frac{4EI}{L} & 0 & -\frac{6EI}{L^2} & \frac{2EI}{L} \\ -\frac{EA}{L} & 0 & 0 & \frac{EA}{L} & 0 & 0 \\ 0 & -\frac{12EI}{L^3} & -\frac{6EI}{L^2} & 0 & \frac{12EI}{L^3} & -\frac{6EI}{L^2} \\ 0 & 6\frac{EI}{L^2} & \frac{2EI}{L} & 0 & -\frac{6EI}{L^2} & \frac{4EI}{L} \end{bmatrix},$$

$$K_{\sigma,N_1} = N_1 \cdot \begin{bmatrix} \frac{1}{2l} & 0 & 0 & -\frac{1}{2l} & 0 & 0 \\ 0 & \frac{3\left(Al^2+10I\right)}{5Al^3} & \frac{4I}{Al^2} & 0 & -\frac{3\left(Al^2+10I\right)}{5Al^3} & \frac{Al^2+20I}{10Al^2} \\ 0 & \frac{4I}{Al^2} & \frac{Al^2+30I}{10Al} & 0 & -\frac{4I}{Al^2} & \frac{60I-Al^2}{60Al} \\ -\frac{1}{2l} & 0 & 0 & \frac{1}{2l} & 0 & 0 \\ 0 & -\frac{3\left(Al^2+10I\right)}{5Al^3} & -\frac{4I}{Al^2} & 0 & \frac{3\left(Al^2+10I\right)}{5Al^3} & -\frac{Al^2+20I}{10Al^2} \\ 0 & \frac{Al^2+20I}{10Al^2} & \frac{60I-Al^2}{60Al} & 0 & -\frac{Al^2+20I}{10Al^2} & \frac{Al^2+30I}{30Al} \end{bmatrix},$$

$$K_{\sigma,N_2} = N_2 \cdot \begin{bmatrix} \frac{1}{2l} & 0 & 0 & -\frac{1}{2l} & 0 & 0 \\ 0 & \frac{3\left(Al^2+10I\right)}{5Al^3} & \frac{Al^2+20I}{10Al^2} & 0 & -\frac{3\left(Al^2+10I\right)}{5Al^3} & \frac{4I}{Al^2} \\ 0 & \frac{Al^2+20I}{10Al^2} & \frac{Al^2+30I}{10Al} & 0 & -\frac{Al^2+20I}{10Al^2} & \frac{60I-Al^2}{60Al} \\ -\frac{1}{2l} & 0 & 0 & \frac{1}{2l} & 0 & 0 \\ 0 & -\frac{3\left(Al^2+10I\right)}{5Al^3} & -\frac{Al^2+20I}{10Al^2} & 0 & \frac{3\left(Al^2+10I\right)}{5Al^3} & -\frac{4I}{Al^2} \\ 0 & \frac{4I}{Al^2} & \frac{60I-Al^2}{60Al} & 0 & -\frac{4I}{Al^2} & \frac{Al^2+30I}{10Al} \end{bmatrix},$$

$$K_{\sigma,M_1} = M_1 \cdot \begin{bmatrix} 0 & -\frac{1}{l^2} & -\frac{1}{l} & 0 & \frac{1}{l^2} & 0 \\ -\frac{1}{l^2} & 0 & 0 & \frac{1}{l^2} & 0 & 0 \\ -\frac{1}{l} & 0 & 0 & \frac{1}{l} & 0 & 0 \\ 0 & \frac{1}{l^2} & \frac{1}{l} & 0 & -\frac{1}{l^2} & 0 \\ \frac{1}{l^2} & 0 & 0 & -\frac{1}{l^2} & 0 & 0 \\ 0 & 0 & 0 & 0 & 0 & 0 \end{bmatrix},$$

$$K_{\sigma,M_2} = M_2 \cdot \begin{bmatrix} 0 & \frac{1}{l^2} & 0 & 0 & -\frac{1}{l^2} & \frac{1}{l} \\ \frac{1}{l^2} & 0 & 0 & -\frac{1}{l^2} & 0 & 0 \\ 0 & 0 & 0 & 0 & 0 & 0 \\ 0 & -\frac{1}{l^2} & 0 & 0 & \frac{1}{l^2} & -\frac{1}{l} \\ -\frac{1}{l^2} & 0 & 0 & \frac{1}{l^2} & 0 & 0 \\ \frac{1}{l} & 0 & 0 & -\frac{1}{l} & 0 & 0 \end{bmatrix}, \tag{A.1}$$

where K_{σ,N_1} and K_{σ,N_2} are the axial force stiffness matrices and K_{σ,M_1} and K_{σ,M_2} are the bending moment stiffness matrices. K_e is the elasticity stiffness matrix.

Conflict of Interests

The authors declare that there is no conflict of interests regarding the publication of this paper.

Acknowledgments

This study was supported by the State High-Tech Research and Development Plans (863), Grant no. 2014AA110402, the Project of the National Key Technology R&D Program in the 12th Five-Year Plan of China (Grant no. 2012BAJ11B01), the Fundamental Research Funds for the Central Universities, and the State Meteorological Administration Special Funds of Meteorological Industry Research (Grant no. 201306102).

References

[1] H. M. Irvine and T. K. Caughey, "The linear theory of free vibrations of a suspended cable," *Proceedings of the Royal Society of London Series A: Mathematical and Physical Sciences*, vol. 341, no. 1626, pp. 299–315, 1974.

[2] M. Irvine and H. M. Irvine, *Cable Structures, Volume 5*, Dover Publications, New York, NY, USA, 1992.

[3] B. H. Kim, T. Park, H. Shin, and T. Y. Yoon, "A comparative study of the tension estimation methods for cable supported bridges," *International Journal of Steel Structures*, vol. 7, no. 1, pp. 77–84, 2007.

[4] Y. Q. Ni, J. M. Ko, and G. Zheng, "Dynamic analysis of large-diameter sagged cables taking into account flexural rigidity," *Journal of Sound and Vibration*, vol. 257, no. 2, pp. 301–319, 2002.

[5] H. Zui, T. Shinke, and Y. Namita, "Practical formulas for estimation of cable tension by vibration method," *Journal of Structural Engineering*, vol. 122, no. 6, pp. 651–656, 1996.

[6] W.-X. Ren, G. Chen, and W.-H. Hu, "Empirical formulas to estimate cable tension by cable fundamental frequency," *Structural Engineering and Mechanics*, vol. 20, no. 3, pp. 363–380, 2005.

[7] G. Ricciardi and F. Saitta, "A continuous vibration analysis model for cables with sag and bending stiffness," *Engineering Structures*, vol. 30, no. 5, pp. 1459–1472, 2008.

[8] D. Dan, Y. Chen, and X. Yan, "Determination of cable force based on the corrected numerical solution of cable vibration frequency equations," *Structural Engineering and Mechanics*, vol. 50, no. 1, pp. 37–52, 2014.

[9] R. Geier, G. De Roeck, and R. Flesch, "Accurate cable force determination using ambient vibration measurements," *Structure and Infrastructure Engineering*, vol. 2, no. 1, pp. 43–52, 2006.

[10] B. H. Kim and T. Park, "Estimation of cable tension force using the frequency-based system identification method," *Journal of Sound and Vibration*, vol. 304, no. 3–5, pp. 660–676, 2007.

[11] Z. Liwen, H. Hua, C. Qingzhi, Z. Jianting, and N. Jincheng, "Cable parameter identification with absorber based on PSO algorithm," *Journal of Chongqing Jiaotong University (Natural Science)*, vol. 2, article 007, 2012.

[12] K. Sun, Y. Zhao, and H. Hu, "Identification of temperature-dependent thermal-structural properties via finite element model updating and selection," *Mechanical Systems and Signal Processing*, vol. 52-53, no. 1, pp. 147–161, 2015.

[13] H. Tabatabai and A. B. Mehrabi, "Design of mechanical viscous dampers for stay cables," *Journal of Bridge Engineering*, vol. 5, no. 2, pp. 114–123, 2000.

[14] S. Krenk, "Vibrations of a taut cable with an external damper," *Transactions ASME—Journal of Applied Mechanics*, vol. 67, no. 4, pp. 772–776, 2000.

[15] S. Krenk, "Complex modes and frequencies in damped structural vibrations," *Journal of Sound and Vibration*, vol. 270, no. 4-5, pp. 981–996, 2004.

[16] J. A. Main and N. P. Jones, "Vibration of tensioned beams with intermediate damper. I: formulation, influence of damper location," *Journal of Engineering Mechanics*, vol. 133, no. 4, pp. 369–378, 2007.

[17] J. A. Main and N. P. Jones, "Vibration of tensioned beams with intermediate damper. II: damper near a support," *Journal of Engineering Mechanics*, vol. 133, no. 4, pp. 379–388, 2007.

[18] Y. Shi and R. Eberhart, "A modified particle swarm optimizer," in *Proceedings of the 1998 IEEE International Conference on Evolutionary Computation, 1998 IEEE World Congress on Computational Intelligence*, pp. 69–73, IEEE, May 1998.

[19] I. C. Trelea, "The particle swarm optimization algorithm: convergence analysis and parameter selection," *Information Processing Letters*, vol. 85, no. 6, pp. 317–325, 2003.

[20] T. Niknam and B. Amiri, "An efficient hybrid approach based on PSO, ACO and k-means for cluster analysis," *Applied Soft Computing Journal*, vol. 10, no. 1, pp. 183–197, 2010.

[21] Z.-H. Zhan, J. Zhang, Y. Li, and Y.-H. Shi, "Orthogonal learning particle swarm optimization," *IEEE Transactions on Evolutionary Computation*, vol. 15, no. 6, pp. 832–847, 2011.

[22] N. J. Cheung, X.-M. Ding, and H.-B. Shen, "OptiFel: a convergent heterogeneous particle swarm optimization algorithm for Takagi-Sugeno fuzzy modeling," *IEEE Transactions on Fuzzy Systems*, vol. 22, no. 4, pp. 919–933, 2014.

[23] Z.-H. Zhan, J. Zhang, Y. Li, and H. S.-H. Chung, "Adaptive particle swarm optimization," *IEEE Transactions on Systems, Man, and Cybernetics, Part B: Cybernetics*, vol. 39, no. 6, pp. 1362–1381, 2009.

[24] E. S. Peer, F. van den Bergh, and A. P. Engelbrecht, "Using neighbourhoods with the guaranteed convergence PSO," in *Proceedings of the IEEE Swarm Intelligence Symposium (SIS '03)*, pp. 235–242, IEEE, August 2003.

[25] W. B. Langdon and R. Poli, "Evolving problems to learn about particle swarm and other optimisers," in *Proceedings of the IEEE Congress on Evolutionary Computation (CEC '05)*, vol. 1, pp. 81–88, September 2005.

[26] K. J. Bathe and E. L. Wilson, *Numerical Methods in Finite Element Analysis*, Prentice-Hall, 1976.